2015

Overcoming the structural versus energy dissipation trade-off in highly crosslinked polymer networks: Ultrahigh strain rate response in polydicyclopentadiene

Daniel B. Knorr Jr.
U.S. Army Research Laboratory, Aberdeen Proving Ground, MD

Kevin A. Masser
U.S. Army Research Laboratory, Aberdeen Proving Ground, MD

Robert M. Elder
U.S. Army Research Laboratory, Aberdeen Proving Ground, MD

Timothy W. Sirk
U.S. Army Research Laboratory, Aberdeen Proving Ground, MD

Mark D. Hindenlang
U.S. Army Research Laboratory, Aberdeen Proving Ground, MD

See next page for additional authors

Composites Science and Technology 114 (2015) 17–25

Contents lists available at ScienceDirect

Composites Science and Technology

journal homepage: www.elsevier.com/locate/compscitech

Overcoming the structural versus energy dissipation trade-off in highly crosslinked polymer networks: Ultrahigh strain rate response in polydicyclopentadiene

Daniel B. Knorr Jr., Kevin A. Masser, Robert M. Elder, Timothy W. Sirk, Mark D. Hindenlang, Jian H. Yu, Adam D. Richardson, Steven E. Boyd, William A. Spurgeon, Joseph L. Lenhart *

U.S. Army Research Laboratory, Aberdeen Proving Ground, MD 21005, United States

ARTICLE INFO

Article history:
Received 9 October 2014
Received in revised form 29 January 2015
Accepted 26 March 2015
Available online 2 April 2015

Keywords:
A. Polymers
A. Amorphous materials
B. Fracture toughness
B. Matrix cracking
B. Impact behavior

ABSTRACT

Ballistic performance, at effective strain rates of (10^4–10^5 s^{-1}), for polymeric dicyclopentadiene (pDCPD) was compared with two epoxy resin/diamine systems with comparable glass transition temperatures. The high rate response was characterized in terms of a projectile penetration kinetic energy, KE_{50}, which describes the projectile kinetic energy at a velocity with a 50% probability of sample penetration. pDCPD showed superior penetration resistance, with a 300–400% improvement in ballistic energy dissipation, when compared with the structural epoxy resins. In addition, unlike typical highly crosslinked networks that become brittle at low temperatures, the improved pDCPD performance occurred over a very broad temperature range (−55 to 75 °C), despite exhibiting a glass transition temperature characteristic of structural resins (~142 °C). In addition to the high T_g, pDCPD exhibited a room temperature glassy storage modulus of 1.7 GPa, offering the potential to circumvent the common structural versus energy dissipation trade-off encountered with conventional crosslinked polymers. Quasi-static measurements suggested that the performance of pDCPD is phenomenologically related to higher fracture toughness and lower yield stress relative to typical epoxies, while molecular dynamics simulations suggest the origin is the lack of strong non-covalent interactions and the facile formation of nanoscale voids to accommodate strain in pDCPD.

Published by Elsevier Ltd.

1. Introduction

High strain rate mechanical performance is increasingly important for light weight protective equipment in military, aerospace, transportation, and construction industries, where crosslinked epoxies are often employed as resins in fiber reinforced polymer composites (FRPC). High strain rate impact events involve complex compressive, tensile, and shear stress states, multi-mode failure processes, elastic deformation, as well as kinetic energy transfer to the composite [1,2]. Interestingly, with FRPCs, energy dissipation in the polymer matrix alone can be responsible for 20–35% of the total energy dissipation [3], however, few studies have focused on improving high rate dissipative capabilities of matrix-only performance in ballistic environments [4]. Epoxy resins that have high stiffness and strength required for structural applications are heavily exploited in fiber reinforced composites, but they are notoriously brittle [5]. Ideally, an epoxy resin would have high stiffness and high T_g while having the ability to dissipate energy over a broad range of temperatures and strain rates.

Along these lines, ballistic characterization of polymers with high velocity projectiles typically results in effective strain rates of 10^4–10^5 s^{-1} and has proven to be an appropriate approach for assessing the high rate energy dissipation capability in polymeric materials [6,7]. One way to quantify this high rate dissipation is to measure the V_{50}, which is the velocity at which there is a 50% probability of penetrating an aluminum foil witness target behind the sample due to transfer of fragments (i.e., spall), or complete penetration of the sample and witness target by the incoming projectile. V_{50} and its kinetic energy related analogue, KE_{50} ($KE_{50} = \frac{1}{2}mV_{50}^2$, where m is the projectile mass), have proved useful in the understanding of the dissipative capability of metals [8] and polymeric composites [9].

Previous work [6] has shown that, for a variety of epoxy resins, the difference between the measurement temperature (T) and the glass transition temperature (T_g), i.e., T–T_g, is important in determining the overall energy dissipation ability of epoxy resins at high strain rates. Specifically, epoxy resins with T_g values approximately

* Corresponding author.
E-mail address: joseph.l.lenhart.civ@mail.mil (J.L. Lenhart).

http://dx.doi.org/10.1016/j.compscitech.2015.03.021
0266-3538/Published by Elsevier Ltd.

30 °C above room temperature showed the best ability to dissipate energy at ballistic strain rates [6]. A subsequent study showed that epoxy resins with nanoscale structure composed of glassy and rubbery domains also provided improved ballistic performance [7], but with some compromise in structural parameters such as temperature dependent stiffness. These works highlight a fundamental trade-off that exists in epoxy resins between structural performance and energy dissipation. A clear need exists for new materials to circumvent this trade-off.

Along these lines, polydicyclopentadiene (pDCPD) is a promising candidate. Crosslinked pDCPD is known for its high toughness [10], high impact strength, and high T_g [11]. pDCPD can be formed by ring-opening metathesis polymerization utilizing a ruthenium-based Grubbs catalyst [12]. Two types of reactions are catalyzed in this method: (i) linear propagation by opening of the highly strained ring followed by (ii) crosslinking by opening of the hexahydropentalene ring. Applications of pDCPD have included self-healing systems of adhesives [13], polymers [14,15], and composites [16].

In this work, we compare the ballistic performance, mechanical properties, and molecular dynamics simulations of pDCPD with two model amine cured epoxy resins with glass transition temperatures similar to pDCPD, which represent various design alternatives when selecting a matrix material for fiber reinforced composites. We show that the ballistic performance of pDCPD is very high despite its high T_g and stiffness, offering the potential for pDCPD based composites to overcome the conventional structural/resin energy dissipation trade-off. We further provide molecular dynamics simulation evidence suggesting that the superior performance of pDCPD is attributed to a lack of strong non-covalent interactions in the cross-linked network and facile nanoscale void formation in response to strain.

2. Experimental

2.1. Materials

Materials used in this study are illustrated in Fig. 1. Dicyclopentadiene (DCPD, >96%, solid at room temperature), 1st generation Grubbs catalyst, and triphenylphosphine were purchased from Sigma Aldrich. Diglycidyl ether of bisphenol A (DGEBA) was obtained from Miller–Stephenson. Polypropylene oxide based-Jeffamine diamine D-230, having a molecular weight of approximately 230 g/mol, was provided by Huntsman. Cyclic diamine curing agent 4,4′-methylenebis(cyclohexylamine) (PACM) was provided by Air Products. All epoxies, curing agents, and DCPD were used as received without further purification. Formulations of epoxy resins were stoichiometric mixtures in all cases.

A typical batch of pDCPD for V_{50}BL(P), dynamic mechanical analysis, and quasi-static mechanical property measurements consisted of 330 g of DCPD with 0.655 g of triphenylphosphine added as an inhibitor [17] to slow the reaction and allow for handling time. This mixture was preheated to 50 °C in an oven purged with nitrogen gas. Separately, 0.41 g of 1st generation Grubb's catalyst was weighed out in a glove box under an inert atmosphere, where it was stored while not in use. Thereafter, it was removed from the glove box and dissolved in 9 mL of toluene. This mixture was then added to the DCPD/triphenylphosphine and was stirred until homogeneous, typically around 30 s. Then, the mixture was poured into molds to cure in an oven purged with nitrogen. The cure cycle for the pDCPD was 4 h at 50 °C followed by 12 h at 175 °C. Epoxy samples were prepared according to a method previously described [6].

2.2. KE_{50} measurement

Ballistic impacts were carried out with a 0.22 caliber gas gun at various temperatures according to a previously described procedure [6]. The kinetic energy (KE_{50}) associated with the V_{50} was then calculated. Values of KE_{50} were normalized to the room temperature value observed for DGEBA/PACM resin. For V_{50} measurements at temperatures above or below room temperature, the targets were tested in an environmental chamber (Instron 3119-410). The targets were equilibrated at the elevated temperatures for 24 h under nitrogen gas purge before testing. For selected V_{50} ballistic events, high speed videography was performed. The camera was placed behind the target fixture, and the frame rate was set at 100,000 frames per second.

2.3. Thermomechanical characterization

Dynamic mechanical analysis (DMA) was performed using a TA instruments Q800 using 17 mm single cantilever mode to measure storage modulus, loss modulus and tan δ as described elsewhere [7]. Measurements were performed at a heating rate of 1 °C/min from −100 °C to 200 °C. The glass transition temperature, T_g, was obtained from the peak in the tan δ. Coefficients of thermal expansion were measured using thermomechanical analysis (TMA) on a Q400 thermomechanical analyzer (TA Instruments, New Castle, DE, USA) using a heat–cool–heat protocol (−60 °C to T_g + 50 °C, 3 °C per minute), and the sample was first heated to its post cure temperature to eliminate previous thermal history.

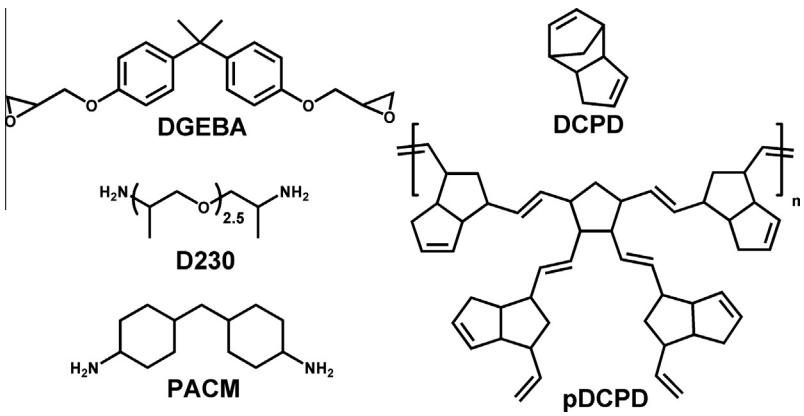

Fig. 1. Epoxy resins diglycidyl ether of bisphenol A (DGEBA), curing agents 4,4′-methylenebis(cyclohexylamine) (PACM), Jeffamine D-230, and DCPD with an illustration of pDCPD with a single, central crosslink.

2.4. Quasi-static mechanical property measurements

Testing to determine the fracture toughness of epoxy resins and pDCPD adhered to ASTM D5045-99. Specimens were single-edge-notch bending geometry machined to 0.635 cm × 1.27 cm × 12 cm ($B \times W \times L$). The test span was set at 10.16 cm with a cross head speed of 10 mm/min. A pre-crack was generated by tapping with a cryo-frozen razorblade, and care was taken to generate instantly propagated cracks ahead of the razor tip, rather than non-propagated cracks. Tensile properties were measured by preparing samples machined to the dimensions of Type IV specimens according to ASTM D638-10. The cross head speed was set to 5 mm/min and DIC (digital image correlation) was used to obtain strain values for the duration of the test. For compression properties, cylindrical samples 1.27 cm × 1.27 cm were prepared and tested using ASTM D695-10 as a guide. The cross head speed was set to 1.3 mm/min. The densities of the thermosets were measured using a Micrometrics Accupyc 1330 pycnometer.

2.5. Dielectric measurements

Broadband dielectric relaxation spectroscopic (BDRS) measurements of the materials were performed on a Novocontrol Concept 40 dielectric spectrometer, as described previously [7]. Thin films, typically 200–400 μm in thickness, were sputtered with gold/palladium electrodes approximately 30 mm in diameter. Due to its low dielectric loss, a thinner, 50 μm thick pDCPD film was prepared by curing DCPD between two silicon wafers, using 50 μm silica spacers to define the film thickness. All samples were measured isothermally every 2.5° or 5° from −150 °C to 200 or 220 °C. The complex dielectric constant ($\varepsilon^* = \varepsilon' - i\varepsilon''$) was measured from 10 MHz to 10 mHz under an applied potential of 1.5 V. For all dielectric constant/loss values reported, the standard deviation of the measurement is less than 1%.

2.6. Simulation methods

To examine the molecular mechanisms underlying mechanical performance, atomistic molecular dynamics simulations of crosslinked poly(dicyclopentadiene) networks were conducted. Our goal was to construct a model with molecular weight between crosslinks (M_c) similar to the experimental value (670 g/mol), thus we constructed pDCPD networks with six repeat units between crosslinks. To compare with the experimental epoxy networks, we constructed a model consisting of DGEBA crosslinked with PACM and D230. As in our previous work [18,19], five replicas of each network composition were constructed, each with relatively large sizes (~200,000 atoms) to reduce the statistical uncertainty of the calculated properties. The crosslinked networks were constructed in the rubbery state using the Monte Carlo simulated annealing approach [20], then slowly cooled into the glassy state (150 K) using the LAMMPS simulation package [21]. We have described the details of this procedure and the molecular dynamics simulations elsewhere [19,22]. Deformation of the model networks was conducted with uniaxial extension simulations at an engineering strain rate of 10^8 s^{-1} up to 35% strain, and five replica network structures were simulated for a total of 15 samples per network. We modeled strains up to 35% which, while not experimentally observed for the present systems, may be observed locally on the nanoscale within a polymer matrix, as macroscopic failure is dictated by flaws within the samples [23]. Furthermore, we monitored bond energies during deformation and found the maximum values (~100 kJ/mol) were much lower than typical covalent bond dissociation energies (~350–600 kJ/mol), indicating that the simulated networks are not unrealistically stressed. We quantified nanovoids in the simulated systems using the program *trj_cavity* [24] with a grid spacing of 1.4 Å and a requirement that voids are surrounded on all sides.

3. Results and discussion

3.1. DMA results

Fig. 2 provides DMA results for all of the thermosets studied. We begin with a discussion of the DMA data as it provides a context for the future discussion of the ballistic performance as DMA provides: (i) the glass transition temperatures of the materials, (ii) relative indication of the stiffness of the material at room temperature as quantified by the storage modulus, and (iii), when coupled with density data, an indication of the molecular weight between crosslinks in the material. The T_g, defined as the peak in $\tan\delta$ from DMA measurements [25,26], spans a range from 96 °C to 164 °C, depending on the thermoset. All T_g values are well above room temperature. For each resin, the molecular weight between crosslinks, M_c, was estimated using the theory of rubber elasticity, where [27]:

$$M_c = \frac{3\rho RT}{E_r} \tag{1}$$

Here, E_r is the minimum storage modulus in the rubbery region from the DMA results, R is the gas constant, T is the absolute temperature at the minimum storage modulus, and ρ is the density of the thermoset at this temperature. The density of the material obtained at room temperature was corrected to the appropriate temperature value using the measured coefficient of linear thermal expansion (COTE) as a function of temperature from TMA measurements, assuming the material is isotropic. As shown in Table 1, the estimated molecular weight between crosslinks is about 670 g/mol for pDCPD, about 550 g/mol for DGEBA/D230 and about 370 g/mol for DGEBA/PACM. Rubber elasticity theory is not strictly valid for highly crosslinked systems, so this will be dubbed the apparent molecular weight between crosslinks, or $M_{c,a}$. These values are qualitative, but have compared favorably with other empirical methods [27] and provide insight into reasons for the ballistic responses observed below. Theoretical values of M_c for epoxies can also be calculated from stoichiometry, i.e., $M_{c,S}$, assuming full conversion using the equation suggested by Crawford and Lesser [28]. For DGEBA/D230 and DGEBA/PACM, values of $M_{c,S}$ are 470 g/mol and 460 g/mol, respectively. Clearly, these theoretical results are different from those obtained by measurement and use of rubber elasticity theory. Specifically, the DGEBA/PACM value estimated from measurements is lower than the calculated value, while that for DGEBA/D230 is higher than the calculated value. The reason for the differences between theoretical and experimental values here is likely caused by the difference in stiffness between the PACM and the D230 monomers, although potential differences in defect structure such as loops, or dangling ends could also contribute. As shown in Fig. 1, PACM has cyclic moieties, which reduces the overall flexibility of the monomer, while D230 is much more linear, and may therefore show more flexibility. This difference can increase the calculated $M_{c,a}$ for DGEBA/D230, while decreasing that of DGEBA/PACM. Interestingly, the pDCPD network structure shown in Fig. 1 and hypothesized in previous work [29] contains carbon–carbon double bonds and bulky pendant hexahydropentalene functionality in the chains that bridge the crosslinking junction points, which will increase the chain stiffness and reduce the $M_{c,a}$ calculated from Eq. (1). Qualitative comparisons of $M_{c,a}$ calculated from rubber elasticity coupled with analysis of the relative chain stiffness suggests that the spacing between crosslinking junction points is larger for the pDCPD networks compared to the epoxies. Since the T_g of a thermoset is influenced by plasticizers and crosslink density, as well as chain and crosslinking junction point stiffness, the high T_g

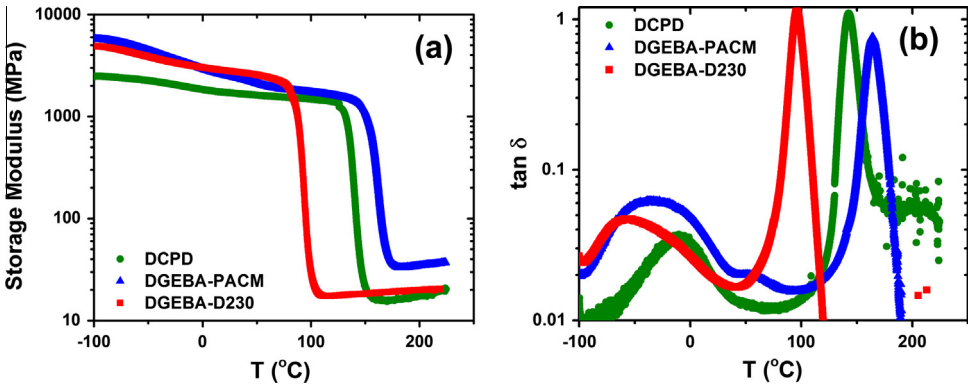

Fig. 2. DMA results for thermosets studied: (a) storage modulus as a function of temperature and (b) tan δ as a function of temperature.

Table 1
Summary of DMA, TMA and density results.

	T_g (°C)	E' at 25 °C (MPa)	E' at $T_g - 50$ °C (MPa)	E' at $T_g + 50$ °C (MPa)	Glassy COTE μm/(m °C)	Rubbery COTE μm/(m °C)	Density at RT (g/cm^3)	Density at $T_g + 50$ °C (g/cm^3)	M_c (g/mol)
pDCPD	142 ± 3	1700 ± 90	1500 ± 80	17 ± 1	86 ± 1	201 ± 6	1.041 ± 0.003	0.98 ± 0.02	670 ± 40
DGEBA/PACM	164 ± 3	2470 ± 120	1590 ± 90	36 ± 1	72 ± 3	183 ± 2	1.158 ± 0.004	1.09 ± 0.02	370 ± 20
DGEBA/D230	96 ± 3	2780 ± 150	2270 ± 110	19 ± 1	76 ± 5	202 ± 2	1.156 ± 0.002	1.10 ± 0.02	550 ± 30

of pDCPD is not likely due to high crosslink density, but rather to the overall stiffness of the chains/junction points due to the presence of rings and double bonds, which prevent the flexibility that would be observed from a less rigid polymer.

3.2. KE_{50} results

Measurements of KE_{50} were performed for the three thermosets studied (pDCPD, DGEBA/PACM and DGEBA/D230) at temperatures ranging from −55 °C to 165 °C, corresponding to a typical military low operational temperature range and the glass transition temperature of the DGEBA/PACM system, respectively. In addition, the ballistic performance for each resin was directly compared at room temperature, at T_g, $T_g - 50$ °C, and $T_g - 100$ °C. KE_{50} results for the resins are plotted as a function of T–T_g in Fig. 3(a), and are normalized to that of DGEBA/PACM measured at room temperature, $T = 22$ °C. Within the figure, the results are compared with previous data [6] showing the KE_{50} values for a series of epoxy resins cured with a stoichiometric quantity of various diamines, where the diamine monomer size, functionality, and stiffness were varied in order to manipulate the epoxy T_g.

As shown in Fig. 3(a), the performance of pDCPD well below its T_g is remarkable. pDCPD shows approximately a three to fourfold increase in KE_{50} over the epoxy formations, with a T–T_g range from −200 °C to −100 °C. In contrast, the DGEBA/PACM formulation shows poor performance throughout the temperature range studied, despite having a T_g similar to the pDCPD. The DGEBA/D230 shows poor performance well below its T_g, and improved performance near T_g. Interestingly, the performance of pDCPD degrades as it approaches T_g, presumably due to softening of the material.

In our formulation, pDCPD is catalyzed by the addition of Grubbs catalyst in toluene. This toluene remains in the system after curing, and may provide some plasticizing effect that contributes to the improved ballistic performance. In order to determine if this plasticizing effect has a substantial influence, we performed room temperature ballistic measurements for pDCPD at various volume fractions of toluene of 1.6, 2.8 (base case), and 5.9 vol.%. As shown in Fig. 3(a), these changes had little influence on the KE_{50}. Also, we performed room temperature KE_{50} measurements for DGEBA/D230 and DGEBA/PACM samples with 2.8 vol.% added toluene. As shown in Fig. 3(a), the addition of toluene dropped the T_g of both formulations, and the normalized KE_{50} value

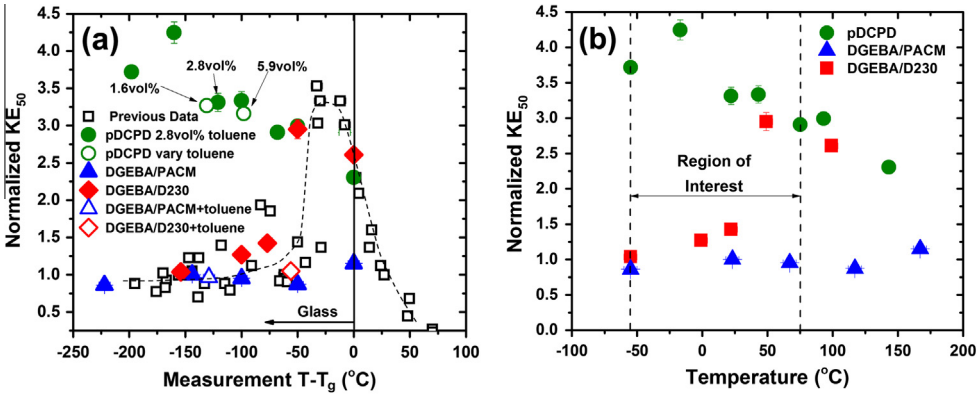

Fig. 3. Plots of normalized KE_{50} as a function of (a) T–T_g and (b) measurement temperature. All previous data taken from [6]. Error in the ballistic KE_{50} and temperature is similar to the symbol size.

of DGEBA/PACM was unchanged, while that of DGEBA/D230 dropped from about 1.4 to about 1.0. Based on these data we conclude that, while the toluene may change the T_g of the pDCPD, it is not expected to have much influence over the ballistic performance at these low concentrations.

A plot of normalized KE50 as a function of measurement temperature is provided in Fig. 3(b). As shown, pDCPD represents the best performance throughout the temperature range studied, and only shows lower performance at relatively high temperatures. Military applications are focused in the region of interest from −55 °C to 75 °C, and, as shown, pDCPD exhibits 300–400% ballistic performance enhancement throughout this entire range in comparison to the epoxy resins studied.

To investigate the ballistic failure process in more detail, we observed the ballistic event using a high speed camera at the V_{50} value for pDCPD, DGEBA/D230, and DGEBA/PACM at room temperature, as shown in Fig. 4(a)–(c), respectively. As shown, the pDCPD sample exhibits only local failure near the impact site without significant cracking or spall, while the DGEBA based formulations show a high degree of cracking that is initiated immediately after impact. Remarkably, the failure behavior of pDCPD is more similar to that of a lower T_g epoxy elastomer previously studied (DGEBA cured with a 2000 g/mol polyether diamine D2000, T_g = −28 °C) [6] than those of the DGEBA/D230 and DGEBA/PACM thermosets, which have more comparable T_g values. Clearly, the high rate mechanical response of pDCPD is very different than typical highly crosslinked epoxy resins.

The failure during ballistic impact is a complex process that involves multi-axial stress states and mixed mode failure behind the projectile impact site. Fracture is apparent in the DGEBA/D230 and DGEBA/PACM samples, not only directly behind the impact site where spall is prevalent, but also with the radial growth of cracks away from impact. In addition, compression directly behind the projectile, coupled with tensile and shear deformations occurring adjacent to the impact site, will also provide penetration resistance. The kinetic energy transfer from the projectile to a "cone" of polymer upon impact is similar for all these systems, as digital image correlation showed minimal back side deformation outside of the spall area directly behind the impact site. The high speed videography in Fig. 4, suggests that fracture resistance in the polymer network is important for ballistic response and that pDCPD is a much tougher material system than typical highly crosslinked epoxy resins.

3.3. Dielectric spectroscopy results

In order to determine if the relaxation dynamics of each system are responsible for the remarkable ballistic performance, the conductivity-free dielectric loss [30] for each of the systems was investigated, as shown in Fig. 5. As with most aliphatic polymers [31], pDCPD is less polar than DGEBA/PACM and DGEBA/D230. The dielectric loss of pDCPD is therefore roughly an order of magnitude less than DGEBA–PACM and DGEBA–D230. Despite the low loss of pDCPD, multiple relaxations were observed. At 1 Hz, pDCPD exhibits three glassy relaxations centered at: approximately −150 °C (labeled δ), approximately −60 °C (labeled γ), and approximately 25 °C (labeled β). Finally, the α relaxation (dynamic T_g) of pDCPD is centered around 175 °C. By comparison, both the DGEBA/PACM and DGEBA/D230 samples exhibit only two relaxations. Both epoxies exhibit a β relaxation, centered at approximately −50 °C and approximately −15 °C for DGEBA/D230 and DGEBA/PACM, respectively. The DGEBA/D230 α relaxation is centered at approximately 100 °C, while the DGEBA/PACM α relaxation is centered at approximately 180 °C.

The temperature dependence of the relaxations shown in Fig. 5 are given in Fig. 6(a) and (b) for the α relaxations and glassy-state relaxations, respectively. At temperatures above approximately 175 °C (i.e., the post-cure temperature of pDCPD), pDCPD begins to further crosslink, which manifests itself as a change in temperature dependence for the α relaxation in Fig. 6(a). This was also observed in the DMA results at similar temperatures. The α relaxations for both the DGEBA–PACM and the DGEBA–D230 epoxies exhibit a classic Vogel–Fulcher–Tammann (Williams–Landel–Ferry) temperature dependence. The temperature dependence of the glassy-state relaxations were modeled with an Arrhenius function, Eq. (2), where f_{Max} is the relaxation frequency, f_o is the frequency prefactor, E_a is the activation energy, R is the universal gas constant, and T is the temperature. The fit parameters are listed in Table 3.

$$f_{Max} = f_o \exp\left(\frac{-E_a}{RT}\right) \tag{2}$$

The β relaxations of pDCPD, DGEBA–PACM, and DGEBA–D230 all likely relate to motion associated with a ring-containing moiety, since ring-flips typically exhibit an activation energy in the 60–80 kJ/mol range [31]. Previous work on epoxy systems has shown that β-relaxation behavior in DGEBA-based epoxies is complex

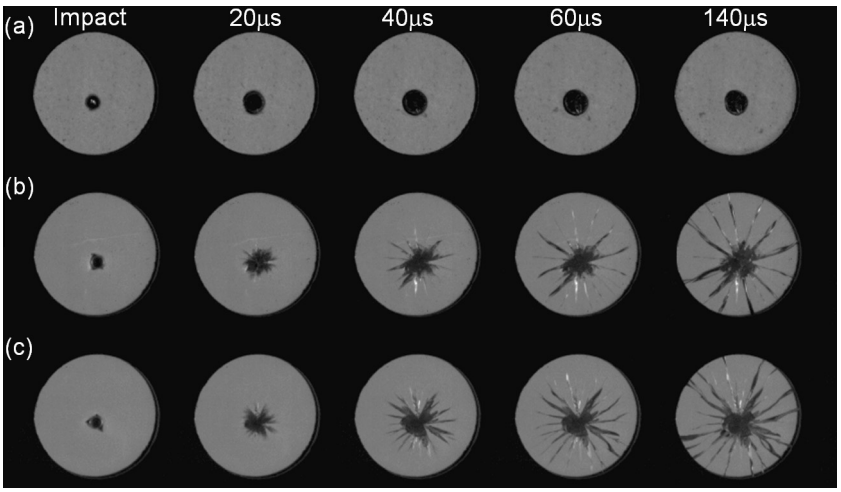

Fig. 4. High speed camera images of the impact event at room temperature for (a) pDCPD, (b) DGEBA/D230, and (c) DGEBA/PACM. Times are listed in the frames, 140 μs was chosen as the final time as all cracks had fully developed for DGEBA/D230 and DGEBA/PACM.

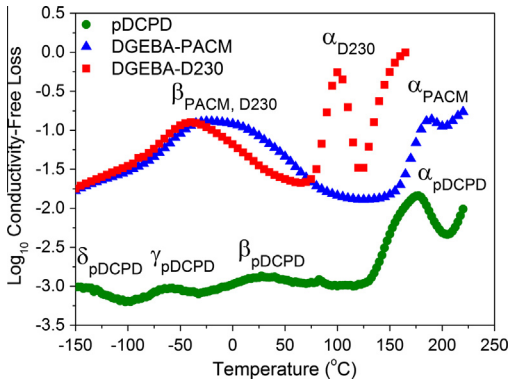

Fig. 5. Conductivity-free dielectric loss for pDCPD (green circles), DGEBA–PACM (blue triangles), and DGEBA–D230 (red squares) as a function of temperature at 1 Hz. (For interpretation of the references to color in this figure legend, the reader is referred to the web version of this article.)

and includes both π flip motion of the phenylene groups and trans–gauche isomerization or other motion of the methylene groups in the hydroxyl ether portion of the cured polymer [32]. The pDCPD β relaxation exhibits a slightly higher activation energy, but it is still in the range of activation energies observed for ring motion. This relaxation could be related to motion of the cyclopentyl crosslinking groups or the uncrosslinked hexahydropentalene groups (see Fig. 1). The pDCPD γ relaxation is caused by the presence of a small amount of confined water, which has an activation energy of roughly 50 kJ/mol in a broad range of systems [33]. Although not shown here, the γ relaxation disappears after high temperature annealing, further suggesting its origins are from confined water. Results for the γ relaxation are shown here to illustrate the state of the pDCPD system under typical curing conditions; it should also be noted that water may also be present in the epoxy resin samples, but is eclipsed by the strength of the β relaxation in those systems. The δ relaxation in pDCPD exhibits a lower activation energy of 32 ± 1 kJ/mol, which is slightly lower than the β relaxation of polybutadiene [34], suggesting the δ relaxation may be related to motions of the short segments between the hexahydropentalene pendant and crosslinked cyclopentane groups of pDCPD.

While these BDRS results sheds light on the relaxation behavior of these systems, the relaxations do not provide an obvious reason for the improved performance of pDCPD relative to the epoxy resins. While the E_a value of the β-relaxation for pDCPD is about 26% higher than those of the epoxies, the tan δ data from the DMA results does not suggest significantly more mechanical energy dissipation in the β-regime compared to the epoxy samples. Our previous work on the ballistic performance of epoxies also suggests β relaxations play a minimal role in highly crosslinked resins [7].

3.4. Quasi-static mechanical property results

Quasi-static compression, tensile and fracture toughness measurements at room temperature and at $T_g - 50$ °C, were performed to gain insight into the rate dependent performance and to identify potential quasi-static indicators of improved ballistic response. The relevant results are summarized in Tables 2 and 3. At room temperature, Table 2, DGEBA/PACM exhibits brittle fracture in tension with a low apparent tensile toughness (integral of stress–strain to failure) of 0.61 MPa. Tensile yield was not observed for the DGEBA/PACM system because this network is so brittle at room temperature that flaws in the tensile specimens dominated the large strain response. In contrast, both DGEBA/D230 and pDCPD yield prior to tensile failure, with similar apparent tensile toughness. However, the DGEBA/D230 exhibits a higher tensile yield stress than pDCPD, while pDCPD shows a higher strain at break than DGEBA/D230. Tensile results for pDCPD are in agreement with the literature [35].

Tensile results at $T_g - 50$ °C are summarized in Table 2. As expected, the modulus values at $T_g - 50$ °C were somewhat lower than at room temperature, but were still sufficiently high to reflect a stiff, glassy polymer. The increased temperature adds sufficient ductility to the DGEBA/PACM system to allow yield to occur, providing a tensile yield stress of 46.4 MPa, which is between that of pDCPD (38.6 MPa) and DGEBA/D230 (55.4 MPa). For both the room temperature and $T_g - 50$ °C tensile measurements, pDCPD exhibited a lower yield stress compared to the epoxies and a necking phenomenon at high strains that was not observed in either epoxy resin, leading to higher elongation to break, which demonstrates an enhanced ability to plastically deform.

In compression at room temperature, DGEBA/PACM did not exhibit a strain softening region after yield, while DGEBA/D230 and pDCPD did, which is likely caused by the variations in effective crosslink density, glassy state density, monomer stiffness, and chain–chain interactions between these networks. The yield stress for pDCPD (73.2 MPa) is in good agreement with previous results [35] and the yield stress for pDCPD is lower than either epoxy. Compression testing results at $T_g - 50$ °C are provided in Table 2. All samples exhibited a strain softening region after yield, with yield strength values of 49.3, 58.1, and 70.2 MPa for pDCPD, DGEBA/PACM and DGEBA/D230, respectively. Similar to the tensile behavior, pDCPD exhibits a lower compressive yield stress than either epoxy formulation.

Fracture toughness results at room temperature are shown in Table 2. As shown, pDCPD is much tougher than either DGEBA/

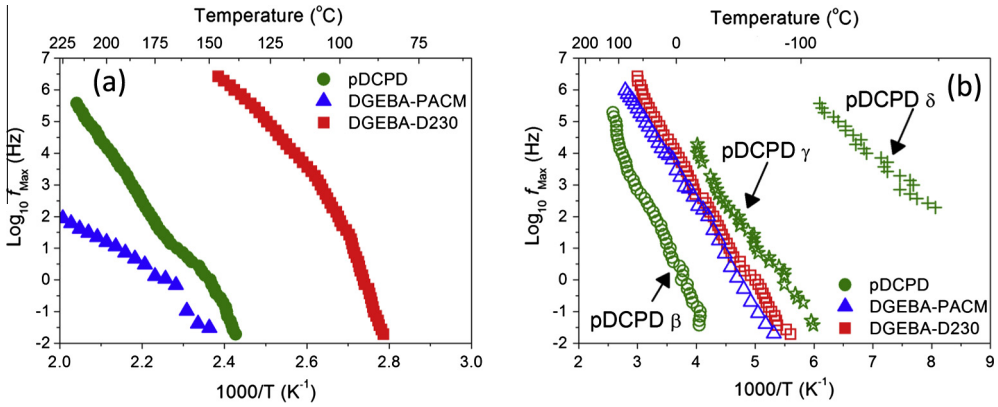

Fig. 6. Arrhenius plots of (a) the segmental relaxations and (b) sub-T_g relaxations for pDCPD (green circles, stars and plus signs), DGEBA–PACM (blue triangles), and DGEBA–D230 (red squares). (For interpretation of the references to color in this figure legend, the reader is referred to the web version of this article.)

Table 2
Mechanical properties of thermosets measured at 22 °C and $T_g - 50$ °C.

Curing agent	T (°C)	KE_{50}	Compressive yield strength (MPa)	Ultimate tensile strength (MPa)	Tensile yield strength (MPa)	Strain at break	Tensile modulus (MPa)	Apparent tensile toughness (MPa)	K_{IC} (MPa $m^{1/2}$)	G_{IC} (kJ/m^2)
pDCPD	22 ± 3	3.31 ± 0.12	73.2 ± 0.8	35.3 ± 2.5	52.4 ± 2.7	0.16 ± 0.03	1770 ± 90	6.1 ± 1.3	2.19 ± 0.15	2.07 ± 0.28
DGEBA/D230	22 ± 3	1.42 ± 0.03	93.6 ± 0.5	56.7 ± 4.4	70.2 ± 5.8	0.11 ± 0.02	3060 ± 170	6.2 ± 1.3	0.76 ± 0.08	0.20 ± 0.02
DGEBA/PACM	22 ± 3	1.00 ± 0.05	115.6 ± 2.3	40.5 ± 3.9	N/A	0.026 ± 0.004	2140 ± 70	0.61 ± 0.16	0.69 ± 0.05	0.19 ± 0.03
pDCPD	$T_g - 50$	2.99 ± 0.07	49.3 ± 1.6	23.6 ± 1.6	38.6 ± 2.5	0.13 ± 0.02	1750 ± 170	3.4 ± 0.4	2.31 ± 0.18[a]	4.57 ± 0.4[a]
DGEBA/D230	$T_g - 50$	2.95 ± 0.13	70.2 ± 1.6	37.8 ± 2.2	55.4 ± 3.0	0.09 ± 0.02	2630 ± 200	3.6 ± 0.6	0.98 ± 0.22	0.50 ± 0.2
DGEBA/PACM	$T_g - 50$	0.87 ± 0.04	58.1 ± 1.0	42.7 ± 1.7	46.4 ± 0.9	0.078 ± 0.014	1760 ± 110	2.9 ± 0.6	0.91 ± 0.05	0.41 ± 0.03

[a] pDCPD samples tore during fracture toughness test and are not strictly valid based on ASTM D5045-99.

Table 3
Arrhenius fitting parameters for the glassy-state relaxations for pDCPD, DGEBA–PACM, and DGEBA–D230.

Relaxation	Activation energy [E_a] (kJ/mol)	Frequency prefactor [f_o] (Hz)
pDCPD β	76 ± 2	$10^{15 \pm 1}$
DGEBA–PACM β	59 ± 1	$10^{15 \pm 1}$
DGEBA–D230 β	60 ± 1	$10^{15 \pm 1}$
pDCPD γ	50 ± 1	$10^{14 \pm 1}$
pDCPD δ	32 ± 1	$10^{15 \pm 1}$

D230 or DGEBA/PACM. It should be noted also that the pDCPD exhibited a "tearing" type behavior during the fracture toughness measurement, which gave the load displacement curve a remarkable tail after the peak load. This is in contrast to the DGEBA formulations, which showed increased load followed quickly by fracture. The pDCPD fracture toughness test was valid according to ASTM D5045-99 at room temperature, due to the low deviation from linearity of the force displacement response near peak load. However, the extended tail after peak load suggests that the pDCPD exhibits tremendous ductility. Finally, fracture toughness values at $T_g - 50$ °C are provided in Table 2. At $T_g - 50$ °C, the fracture toughness test for pDCPD does not meet ASTM D5045-99 standards as a valid test. The fracture toughness for DGEBA/D230 increased somewhat at $T_g - 50$ °C to 0.98 MPa $m^{1/2}$ from 0.76 MPa $m^{1/2}$ at room temperature; similarly, that of DGEBA/PACM also increased, from 0.69 at room temperature to 0.91 MPa $m^{1/2}$ at $T_g - 50$ °C. Again, both DGEBA/D230 and DGEBA/PACM still show conventional brittle failure, characteristic of highly crosslinked epoxy resins, while pDCPD exhibited substantial tearing behavior, and demonstrated a more ductile response.

At room temperature, the normalized KE_{50} values for pDCPD, DGEBA/D230 and DGEBA/PACM are 3.31, 1.42 and 1.0, respectively (Table 2 and Fig. 3). Looking at the quasi-static results, the significant differences that may account for the remarkable behavior of pDCPD relative to the DGEBA formulations are (i) the very high fracture toughness, (ii) the relatively low tensile yield stress, and (iii) the relatively low compressive yield stress. That is, during a ballistic event, pDCPD readily yields in tension in regions adjacent to the impact site and in compression in the region behind the impact site, followed by plastic deformation. Furthermore, the high pDCPD fracture toughness discourages spall and radial fracture propagation, which means that all energy dissipation is routed to the plastic deformation of the material.

At $T_g - 50$ °C, the normalized KE_{50} values for pDCPD, DGEBA/D230 and DGEBA/PACM are 2.99, 2.95 and 0.87, respectively (Table 2 and Fig. 3). In contrast to room temperature, the KE_{50} of pDCPD decreased somewhat, that of DGEBA/PACM is approximately the same, and that of DGEBA/D230 increased dramatically. The decrease in KE_{50} for pDCPD is likely due to the softening of the material as evidenced by the lower yield stress values. Comparing the quasi-static and ballistic results at both room temperature and $T_g - 50$ °C suggests that an optimal yield stress is required for good ballistic performance. Failure during ballistic impact is a complicated phenomenon with multi-axial stress states, mixed mode failure processes, temperature and pressure dependent mechanical response, and a broad range of effective local strain rates. Therefore, the quasi-static results can shed only qualitative insight into the penetration resistance. As such, we performed molecular dynamics simulations to gain insight into the difference in mechanical properties between pDCPD and the epoxy resins.

3.5. Molecular simulation results

A pDCPD network with six un-crosslinked monomers between crosslink points (similar to the experimental system), DGEBA/PACM, and DGEBA/D230 epoxy networks were modeled using atomistic molecular dynamics to study the molecular origins of the experimental observations.

We first studied the role of inter-chain interactions during deformation by monitoring the electrostatic potential energy (i.e., the work required to overcome electrostatic interactions to achieve a particular strain), which captures the effect of hydrogen-bonds, dipole–dipole attractions, and attraction of the atomic partial charges. The pDCPD networks show a negligible increase in electrostatic energy with increasing strain, while for the DGEBA/PACM and DGEBA/D230 networks, the energy increases substantially, Fig. 7(a). This result supports the idea that strong non-covalent interactions in epoxy resist deformation, thus leading to more brittle behavior, higher modulus, and higher yield strengths, as were observed in the quasi-static experimental data discussed above.

Recent research [36] has suggested that nanoscale void behavior is related to ductility in thermoset systems. To examine the role of nanovoids in determining the mechanical properties of pDCPD and epoxy networks, we quantified and characterized nanovoids during deformation of the crosslinked polymers. Fig. 7(b) shows the distribution of void sizes at engineering strains of zero (filled symbols) and 0.35 (open symbols), and the nanovoid fraction in the epoxy and pDCPD networks as a function of engineering strain (inset). At zero strain, the epoxy and pDCPD networks have similar void size distributions and nanovoid fractions. As strain increases, the void fractions (inset) increase, in the order of decreasing $M_{c,a}$, i.e., DGEBA/PACM > DGEBA/D230 > pDCPD, which is similar to previous experimental results for voids in networks with varying crosslink density [37]. This indicates that, to locally accommodate higher strains, more nanovoid space is required for the epoxy systems having lower $M_{c,a}$ values, while the high $M_{c,a}$ pDCPD can tolerate high strains with comparatively less void space. Further, the number density distribution at high strains (0.35, open symbols in Fig. 7(b)) show that epoxies have a larger distribution of void sizes (maximum void size of ~7000 $Å^3$) than pDCPD (maximum void size of ~1000 $Å^3$). Ongoing simulation studies are aimed at further exploring this phenomenon.

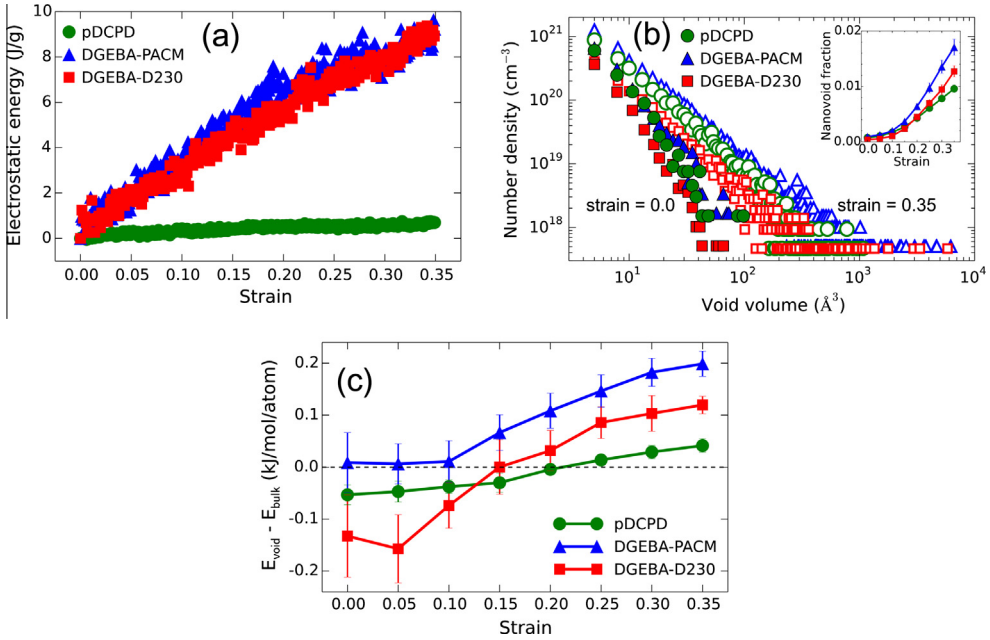

Fig. 7. (a) Change in total electrostatic energy, (b) void volume distribution and (inset) void fraction, and (c) difference in non-bonded interaction energy between atoms near voids and atoms in the bulk polymer for the simulated pDCPD, DGEBA/PACM, and DGEBA/D230 networks as a function of engineering strain at 150 K. Solid and open symbols in (b) are at 0% and 35% strain, respectively.

To explore the relation between non-covalent interactions and voids, we examined the effect of voids on the potential energy of nearby atoms by computing the non-bonded potential energy (i.e., van der Waals and electrostatic energies [38]) for atoms near voids (within 6 Å) and for atoms in the bulk polymer. The energy difference between atoms near voids and in the bulk polymer, i.e., the energetic cost for moving an atom from the bulk to near a void, is shown in Fig. 7(c). For pDCPD, the energy difference is near zero for all strains studied, indicating that it is not unfavorable for atoms to reside near voids. In contrast, the energy difference for epoxies increases rapidly as strain increases, indicating that it becomes unfavorable for atoms to reside near voids under higher strain.

While more research is on-going to elucidate the molecular mechanism of deformation (we are pursuing positron annihilation lifetime spectroscopy measurements to confirm the simulation findings), we postulate a general explanation for the superior performance of pDCPD relative to the epoxy resins based on the experimental and simulation results presented above. The low $M_{c,a}$ values in the epoxies mean that the epoxy networks must develop more nanoscale void volume to accommodate higher strains due to geometric constraints induced by the high crosslink density. However, this void formation is energetically unfavorable in epoxies due to the need to break the strong electrostatic interactions to create or expand a void. Straining the epoxy therefore requires more work, which leads to a higher modulus, a higher yield stress, and embrittlement. In contrast, the higher $M_{c,a}$ of pDCPD requires less nanovoid volume development to accommodate higher strains. Furthermore, void formation in pDCPD at higher strains is energetically neutral due to the lack of strong electrostatic interactions. Therefore, void formation and growth can occur with less work, leading to a lower modulus, a lower yield stress, and more facile plastic deformation.

4. Conclusions

These results demonstrate that pDCPD can circumvent the common structural versus energy dissipation trade-off encountered in highly crosslinked epoxy resin systems, as evidenced by the quasi-static and ballistic comparisons with both DGEBA/PACM and DGEBA/D230 resins. Quasi-static compression, tension and fracture toughness measurements were consistent with ballistic performance in that the pDCPD showed high fracture toughness, low yield strength in tension, and low yield strength in compression. Examination of the relaxation behavior by dielectric spectroscopy and DMA suggested that glassy-state relaxations are not the primary cause of the excellent high strain rate behavior of pDCPD. Further, molecular dynamics simulations of these networks suggest that pDCPD requires less nanovoid volume formation to accommodate strain due to its high $M_{c,a}$, and also lacks the strong non-covalent interactions of the epoxies. Therefore, pDCPD can more easily accommodate higher strains via the development of nanovoids during deformation. This research has important implications for light weight protective materials in a broad range of industries including military, aerospace, transportation, and construction technologies, where pDCPD is becoming a candidate material as a polymer matrix in high performance composite applications. Preliminary results for glass fiber reinforced pDCPD composites (not shown) have demonstrated that the improved bulk resin ballistic performance can translate into improved composite impact performance. However, substantial research is required to exploit pDCPD as a resin in fiber reinforced composites, particularly relative to composite processing and optimization of the fiber–pDCPD resin interface. This is a focus of ongoing research.

Acknowledgements

Funding for this work was provided by the U.S. Army Research Laboratory. This work was supported by grants of computer time from the DOD High Performance Computing Modernization Program at the U.S. Air Force Research Laboratory and U.S. Army Engineer Research and Development Center DoD Supercomputing Resource Centers.

References

[1] Morye SS, Hine PJ, Duckett RA, Carr DJ, Ward IM. Modelling of the energy absorption by polymer composites upon ballistic impact. Compos Sci Technol 2000;60(14):2631–42.

[2] Deka LJ, Bartus SD, Vaidya UK. Damage evolution and energy absorption of E-glass/polypropylene laminates subjected to ballistic impact. J Mater Sci 2008;43(13):4399–410.
[3] Zee RH, Hsieh CY. Energy absorption processes in fibrous composites. Mater Sci Eng, A 1998;246(1–2):161–8.
[4] Naik NK, Shankar PJ, Kavala VR, Ravikumar G, Pothnis JR, Arya H. High strain rate mechanical behavior of epoxy under compressive loading: experimental and modeling studies. Mater Sci Eng, A 2011;528(3):846–54.
[5] Nielsen LE, Landel RF. Mechanical properties of polymers and composites. New York: Marcel Dekker; 1994.
[6] Knorr Jr DB, Yu JH, Richardson AD, Hindenlang MD, McAninch IM, La Scala JJ, et al. Glass transition dependence of ultrahigh strain rate response in amine cured epoxy resins. Polymer 2012;53(25):5917–23.
[7] Masser KA, Knorr Jr DB, Hindenlang MD, Yu JH, Richardson AD, Strawhecker KE, et al. Relating structure and chain dynamics to ballistic performance in transparent epoxy networks exhibiting nanometer scale heterogeneity. Polymer 2015;58:96–106.
[8] Czarnecki GJ. Estimation of the V-50 using semi-empirical (1-point) procedures. Compos Part B – Eng 1998;29(3):321–9.
[9] Gellert EP, Cimpoeru SJ, Woodward RL. A study of the effect of target thickness on the ballistic perforation of glass-fibre-reinforced plastic composites. Int J Impact Eng 2000;24(5):445–56.
[10] Kessler MR, White SR. Cure kinetics of the ring-opening metathesis polymerization of dicyclopentadiene. J Polym Sci Part A – Polym Chem 2002;40(14):2373–83.
[11] Lenhardt JM, Kim SH, Nelson AJ, Singhal P, Baumann TF, Satcher Jr JH. Increasing the oxidative stability of poly(dicyclopentadiene) aerogels by hydrogenation. Polymer 2013;54(2):542–7.
[12] Bielawski CW, Grubbs RH. Living ring-opening metathesis polymerization. Prog Polym Sci 2007;32(1):1–29.
[13] Jin H, Miller GM, Pety SJ, Griffin AS, Stradley DS, Roach D, et al. Fracture behavior of a self-healing, toughened epoxy adhesive. Int J Adhes Adhes 2013;44:157–65.
[14] White SR, Sottos NR, Geubelle PH, Moore JS, Kessler MR, Sriram SR, et al. Autonomic healing of polymer composites. Nature 2001;409(6822):794–7.
[15] Kessler MR, Sottos NR, White SR. Self-healing structural composite materials. Compos A Appl Sci Manuf 2003;34(8):743–53.
[16] Patel AJ, Sottos NR, Wetzel ED, White SR. Autonomic healing of low-velocity impact damage in fiber-reinforced composites. Compos A Appl Sci Manuf 2010;41(3):360–8.
[17] Mauldin TC, Kessler MR. Latent catalytic systems for ring-opening metathesis-based thermosets. J Therm Anal Calorim 2009;96(3):705–13.
[18] Sirk TW, Khare KS, Karim M, Lenhart JL, Andzelm JW, McKenna GB, et al. High strain rate mechanical properties of a cross-linked epoxy across the glass transition. Polymer 2013;54(26):7048–57.
[19] Sirk TW, Karim M, Khare KS, Lenhart JL, Andzelm JW, Khare R. Bi-modal polymer networks: composition-dependent trends in thermal, volumetric and structural properties from molecular dynamics simulation. Polymer 2015;58:199–208.
[20] Lin P-H, Khare R. Molecular simulation of cross-linked epoxy and epoxy–POSS nanocomposite. Macromolecules 2009;42(12):4319–27.
[21] Plimpton S. Fast parallel algorithms for short-range molecular dynamics. J Comput Phys 1995;117(1):1–19.
[22] Jang C-W, Sirk TW, Andzelm JW, Abrams CF. Comparison of crosslinking algorithms in molecular dynamics simulations of thermosetting polymers. Macromol Theory Simul 2015 [in press], http://dx.doi.org/10.1002/mats.201400094.
[23] Pascault J-P, Verdu J, Williams RJJ. Thermosetting polymers. New York: Marcel Dekker; 2002.
[24] Paramo T, East A, Garzón D, Ulmschneider MB, Bond PJ. Efficient characterization of protein cavities within molecular simulation trajectories: trj_cavity. J Chem Theory Comput 2014;10(5):2151–64.
[25] Franco M, Corcuera MA, Gavalda J, Valea A, Mondragon I. Influence of curing conditions on the morphology and physical properties of epoxy resins modified with a liquid polyamine. J Polym Sci, Part B: Polym Phys 1997;35(2):233–40.
[26] Franco M, Mondragon I, Bucknall CB. Blends of epoxy resin with amine-terminated polyoxypropylene elastomer: morphology and properties. J Appl Polym Sci 1999;72(3):427–34.
[27] van der Sanden MCM, Meijer HEH. Deformation and toughness of polymeric systems. 3. Influence of cross-link density. Polymer 1993;34(24):5063–72.
[28] Crawford E, Lesser AJ. The effect of network architecture on the thermal and mechanical behavior of epoxy resins. J Polym Sci, Part B: Polym Phys 1998;36(8):1371–82.
[29] Davidson TA, Wagener KB. The polymerization of dicyclopentadiene: an investigation of mechanism. J Mol Catal A: Chem 1998;133(1–2):67–74.
[30] Wübbenhorst M, van Turnhout J. Analysis of complex dielectric spectra. I. One-dimensional derivative techniques and three-dimensional modelling. J Non-Cryst Solids 2002;305(1–3):40–9.
[31] Kremer F, Schonhals A. Broadband dielectric spectroscopy. Springer; 2003.
[32] Shi JF, Inglefield PT, Jones AA, Meadows MD. Sub-glass transition motions in linear and cross-linked bisphenol-type epoxy resins by deuterium line shape NMR. Macromolecules 1996;29(2):605–9.
[33] Cerveny S, Alegria A, Colmenero J. Universal features of water dynamics in solutions of hydrophilic polymers, biopolymers, and small glass-forming materials. Phys Rev E 2008;77(3).
[34] Casalini R, Ngai KL, Robertson CG, Roland CM. α- and β-relaxations in neat and antiplasticized polybutadiene. J Polym Sci, Part B: Polym Phys 2000;38(14):1841–7.
[35] Constable GS, Lesser AJ, Coughlin EB. Morphological and mechanical evaluation of hybrid organic-inorganic thermoset copolymers of dicyclopentadiene and mono- or tris(norbornenyl)-substituted polyhedral oligomeric silsesquioxanes. Macromolecules 2004;37(4):1276–82.
[36] Mukherji D, Abrams CF. Microvoid formation and strain hardening in highly cross-linked polymer networks. Phys Rev E 2008;78(5):050801.
[37] Soles CL, Chang FT, Bolan BA, Hristov HA, Gidley DW, Yee AF. Contributions of the nanovoid structure to the moisture absorption properties of epoxy resins. J Polym Sci, Part B: Polym Phys 1998;36(17):3035–48.
[38] Sirk TW, Moore S, Brown EF. Characteristics of thermal conductivity in classical water models. J Chem Phys 2013;138(6).